
Research Article: New Research | Development

L-Type Calcium Channels Contribute to Ethanol-Induced Aberrant Tangential Migration of Primordial Cortical GABAergic Interneurons in the Embryonic Medial Prefrontal Cortex

<https://doi.org/10.1523/ENEURO.0359-21.2021>

Cite as: eNeuro 2021; 10.1523/ENEURO.0359-21.2021

Received: 6 September 2021

Revised: 17 November 2021

Accepted: 7 December 2021

This Early Release article has been peer-reviewed and accepted, but has not been through the composition and copyediting processes. The final version may differ slightly in style or formatting and will contain links to any extended data.

Alerts: Sign up at www.eneuro.org/alerts to receive customized email alerts when the fully formatted version of this article is published.

Copyright © 2021 Lee et al.

This is an open-access article distributed under the terms of the Creative Commons Attribution 4.0 International license, which permits unrestricted use, distribution and reproduction in any medium provided that the original work is properly attributed.

1 **Manuscript Title:**

2 L-Type Calcium Channels Contribute to Ethanol-Induced Aberrant Tangential Migration of
3 Primordial Cortical GABAergic Interneurons in the Embryonic Medial Prefrontal Cortex

4

5 **Abbreviated Title:** Calcium, Ethanol, and Migration

6

7 **Author Names and Affiliations:**

8 Stephanie M. Lee, Pamela W.L. Yeh, Hermes H. Yeh

9 Department of Molecular and Systems Biology, Geisel School of Medicine at Dartmouth,
10 Hanover, NH 03755

11

12 **Author contributions:**

13 SML and HHY Designed Research; SML Performed Research; SML Analyzed data; PWLY
14 Provided Resources; SML and HHY Wrote the paper

15

16 **Correspondence should be addressed to:**

17 Hermes H. Yeh, Ph.D.

18 Department of Molecular and Systems Biology

19 Geisel School of Medicine at Dartmouth, Hanover, NH 03755

20 Email: hermesyeh@dartmouth.edu

21

Number of Figures: 6

Number of words for Abstract: 250

Number of Tables: 0

Number of words for Significance Statement: 116

Number of Multimedia: 0

Number of words for Introduction: 730

Number of words for Discussion: 1221

22

23 Acknowledgements: The authors thank Ryan Ding, Michelle Yu, and Victoria Nedder for
24 assisting in data collection and analysis. The authors acknowledge funding from the National
25 Institute on Alcohol Abuse and Alcoholism at the National Institutes of Health PHS NIH R01
26 AA023410, AA027754 to HHY, and F31 AA027694-01 to SML.

27

28 Conflict of Interest: Authors report no conflict of interest.

29

30 Funding sources: PHS NIH R01 AA023410, AA027754, to HHY, and F31 AA027694-01 to SML.

31 **Abstract**

32 Exposure of the fetus to alcohol (ethanol) via maternal consumption during pregnancy
33 can result in fetal alcohol spectrum disorders (FASD), hallmarked by long-term physical,
34 behavioral, and intellectual abnormalities. In our preclinical mouse model of FASD, prenatal
35 ethanol exposure disrupts tangential migration of corticopetal GABAergic interneurons in the
36 embryonic medial prefrontal cortex (mPFC). We postulated that ethanol perturbed the normal
37 pattern of tangential migration via enhancing GABA_A receptor-mediated membrane
38 depolarization that prevails during embryonic development in GABAergic cortical interneurons.
39 However, beyond this, our understanding of the underlying mechanisms is incomplete. Here, we
40 tested the hypothesis that the ethanol-enhanced depolarization triggers downstream an
41 increase in high-voltage activated nifedipine-sensitive L-type calcium channel (LTCC) activity,
42 and provide evidence implicating calcium dynamics in the signaling scheme underlying the
43 migration of embryonic GABAergic interneurons and its aberrance. Tangentially migrating
44 Nkx2.1+ GABAergic interneurons expressed immunoreactivity to Cav1.2, the canonical
45 neuronal isoform of the L-type calcium channel. Prenatal ethanol exposure did not alter its
46 protein expression profile in the embryonic mPFC. However, exposing ethanol concomitantly
47 with the LTCC blocker nifedipine prevented the ethanol-induced aberrant migration both *in vitro*
48 and *in vivo*. In addition, whole-cell patch clamp recording of LTCCs in GABAergic interneurons
49 migrating in embryonic medial prefrontal cortical slices revealed that acutely applied ethanol
50 potentiated LTCC activity in migrating GABAergic interneurons. Based on evidence reported in
51 the present study, we conclude that calcium is an important intracellular intermediary
52 downstream of GABA_A receptor-mediated depolarization in the mechanistic scheme of an
53 ethanol-induced aberrant tangential migration of embryonic GABAergic cortical interneurons.

54

55

56 Significance Statement

57 The etiology of fetal alcohol spectrum disorders (FASD) takes place *in utero* when the
58 fetus is exposed to alcohol. While the outcome of FASD has been well characterized, the
59 mechanism underlying its embryonic etiology is incompletely understood. Here, we investigated
60 the role of L-type voltage-gated calcium channels (LTCCs) in the ethanol-induced aberrant
61 tangential migration of cortical GABAergic interneurons. The findings from our study highlight
62 LTCCs as important regulators underlying the aberrant tangential migration resulting from
63 prenatal ethanol exposure and suggest that they bear therapeutic potential in managing and
64 treating FASD. The results also propose an interplay between chloride and calcium in the
65 migrating embryonic interneurons, and exposure to ethanol may enhance this interaction,
66 contributing to the etiology of FASD.

67

68 Introduction

69 Fetal alcohol spectrum disorders (FASD), hallmarked by lifelong physical, behavioral,
70 and intellectual abnormalities, is the leading cause of preventable neurodevelopmental
71 disorders (American Academy of Pediatrics, 2000; Carr et al., 2010; Mattson et al., 2011).
72 Alcohol (ethanol) readily crosses the placenta, and can be detected in the fetus as well as in the
73 amniotic fluid (Idänpään-Heikkilä et al., 1972; Cuzon et al., 2008). The National Survey on Drug
74 Use and Health reported that, from 2015-2018, drinking prevalence for pregnant women in the
75 past 12 months was 64.7%, current drinking was 9.8%, and current binge drinking was 4.5%
76 (England et al., 2020). Of those respondents in their first trimester of pregnancy, 19.6% reported
77 current alcohol use and 10.5% reported binge drinking. Many women are not aware that they
78 are pregnant until after the 4th or 6th week of pregnancy, increasing the risk of ethanol
79 consumption early in gestation (Floyd et al., 1999). The prevalence of FASD is estimated at
80 33.5 per 1000 live births in the USA, 22.7 globally, and as high as 113.22 in some populations

81 (Roozen et al., 2016). These statistics underscore that FASD is a significant public health
82 concern. Understanding its embryonic etiology is thus critical for managing and treating FASD.

83 We have employed a mouse model of FASD in which pregnant mice consumed ethanol
84 either chronically throughout gestation or in a binge-type pattern to investigate the effects of
85 prenatal ethanol exposure on the development of the cerebral cortex (Cuzon et al., 2008;
86 Skorput et al., 2015; Delatour et al., 2019, 2020). Ethanol exposure *in utero* throughout
87 gestation altered tangential migration of corticopetal GABAergic interneurons, regulated by an
88 ambient level of GABA in the embryonic telencephalon (Cuzon et al., 2006; 2008). Binge-type
89 ethanol exposure also disrupted tangential migration, which was associated with a persistent
90 interneuronopathy that manifested as an excitatory/inhibitory (E/I) imbalance, hyperactivity, and
91 deficits in executive function in young adult mice (Skorput et al., 2015). In a more recent study
92 (Skorput et al., 2019), acute exposure to ethanol enhanced the membrane depolarization
93 mediated through GABA_A receptors expressed in GABAergic interneurons (GINs) migrating in
94 the embryonic telencephalon. This ethanol-induced enhancement was normalized by
95 bumetanide, a blocker of the NKCC1 co-transporter. Co-treatment of pregnant dams with
96 bumetanide and ethanol also mitigated aberrant tangential migration in the short term, as well
97 as interneuronopathy and behavioral deficits in the long term. However, it remained unclear how
98 the potentiation of GABA-mediated depolarization following ethanol exposure disrupted
99 tangential migration. Here, we hypothesized that this ethanol-potentiated depolarization triggers
100 downstream signaling molecules that enhance migration, notably an increase in the activity of
101 voltage-gated calcium channels which, in turn, leads to an abnormally augmented level of
102 tangential migration.

103 Indeed, calcium signaling is a key mechanism underlying neuronal migration, including
104 tangential migration of cortical GINs (Komuro and Rakic, 1996, 1998; Soria and Valdeolmillos,
105 2002; Moya and Valdeolmillos, 2004; Inada et al., 2011). Migrating neurons undergo a wide
106 range of cellular processes, including neurite extension, nucleokinesis, and trailing tail retraction

107 through cytoskeletal dynamics, all of which are regulated by calcium-dependent signaling
108 (Gomez and Spitzer, 1999; Lautermilch and Spitzer, 2000; Gomez et al., 2001; Wen et al.,
109 2004; Kerstein et al., 2017). Calcium influx through voltage-gated L-type calcium channels
110 (LTCCs) has been implicated in various processes of neuronal and non-neuronal migration,
111 including neurite extension and trailing tail retraction (Yang and Huang, 2005; Darcy and
112 Isaacson, 2009; Bortone and Polleux, 2009; Danesi et al., 2018; Kamijo et al., 2018).
113 Neurotransmitters such as glutamate and GABA have been reported to invoke calcium influx
114 through LTCCs (Bortone and Polleux, 2009; Horigane et al., 2019). Furthermore, LTCCs have
115 been linked to neuropsychiatric disorders, including autism spectrum disorders, timothy
116 syndrome and schizophrenia (Cross-Disorder Group of the Psychiatric Genomics Consortium,
117 2013; Kabir et al., 2017; Danesi et al., 2018).

118 In the present study, we tested the hypothesis that an ethanol-induced potentiation of
119 LTCCs contributes to the aberrant tangential migration of GABAergic interneurons. We report
120 here that co-treatment with ethanol and nifedipine, an LTCC blocker, prevented the ethanol-
121 induced aberrant tangential migration both *in vitro* and *in vivo*. In addition, we report that ethanol
122 potentiates LTCC activity in migrating GABAergic interneurons in the embryonic cortex. We
123 conclude that LTCCs play an important role in manifesting the aberrant migration of embryonic
124 GABAergic interneurons induced by prenatal ethanol exposure and propose that they may be
125 potential therapeutic targets for mitigating the teratogenic effects of ethanol on the pathoetiology
126 of FASD.

127

128 **Materials and Methods**

129 *Animals*

130 All procedures were performed in accordance with the National Institutes of Health
131 Guide for the Care and Use of Laboratory Animals and approved by Dartmouth College
132 Institutional Animal Care and Use Committee. The Nkx2.1-Cre transgenic mouse line (originally

133 obtained from Dr. Stewart Anderson; Xu et al., 2008) was crossed with the Ai14 Cre-reporter
134 mouse line (Jackson laboratories, Bar Harbor, ME) to yield Nkx2.1Cre/Ai14 mice harboring
135 tdTomato-fluorescent MGE-derived GABAergic interneurons (referred to as Nkx2.1+ GINs;
136 Skorput et al., 2015). For time-pregnant mating, pairs of male and female mice were housed
137 overnight, with the following day designated as E0.5. Embryonic day 13.5-16.5 embryos were
138 included in this study as available. Based on results of Y-chromosome-specific genotyping
139 (Stratman et al., 2003), no difference in the ratio of male to female offspring was noted between
140 treatment groups. Embryonic days 13.5 - 16.5 were operationally defined to be within the age
141 range roughly equivalent to mid-first trimester in humans (Clancy et al., 2001; Parnell et al.,
142 2014).

143

144 *Ethanol exposure paradigm*

145 This study used the binge-type ethanol exposure paradigm reported in previous studies
146 (Skorput et al., 2015, 2019; Delatour et al., 2019, 2020). Timed-pregnant mice were exposed to
147 ethanol from E13.5 to E16.5, when tangential migration of MGE-derived cortical interneuron is
148 at its peak in mice (Anderson et al., 2001; Batista-Brito and Fishell, 2009; Gelman et al., 2009;
149 Hladnik et al., 2014; Jiménez et al., 2002; Marín and Rubenstein, 2001; Parnavelas, 2000).
150 Pregnant dams were individually housed and fed a liquid diet (Research Diets, New Brunswick,
151 NJ) containing alcohol (5% w/w) or isocaloric control diet containing maltose. Mice were
152 maintained under normal 12/12 hr light/dark cycle and water was available ad libitum. The liquid
153 food was replenished daily between 9:00 and 11:00 AM, when the amount consumed and the
154 weight of the dams were measured. Following termination of the liquid diet on E16.5, the mice
155 were returned to standard chow. Mean dam blood alcohol level (BAL), measured at 11:30 PM
156 on E15.5, was 0.08%, consistent with previous binge ethanol measurements (Skorput et al.,
157 2015, 2019). Blood was collected via tail-vein and assessed using an Analox Instruments GM7
158 series analyzer (Lunenburg, MA). Following the binge-type ethanol consumption paradigm,

159 pregnant dams carried their offspring to full term with no apparent effect on litter size. For
160 nifedipine treatment, nifedipine stock was dissolved in DMSO and added to the control or 5%
161 ethanol-containing liquid food to achieve 0.15 mg of nifedipine per kg body weight of the mice
162 being fed. The final dilution of DMSO in the liquid food was 1:120,000.

163

164 *Organotypic embryonic slice culture*

165 Organotypic culture of embryonic slices was performed as described previously (Cuzon
166 et al., 2006; Skorput et al., 2019). At embryonic day E14.5, time-pregnant dams were
167 asphyxiated using CO₂ and embryos were removed by cesarean section. The tdTomato-
168 expressing embryos were identified using fluorescence UV (Biological Laboratory Equipment
169 Maintenance and Service, Budapest, Hungary). The brains were quickly harvested under a
170 dissecting microscope and immersed in ice-cold slicing media (1:1 F12:DMEM) oxygenated by
171 continuous bubbling with 95% O₂/5% CO₂. The dissected brains were embedded in 3.5% low
172 melting point agarose in 1:1 F12:DMEM, and 250 μm-thick coronal slices were collected using a
173 vibrating microtome (Electron Microscopy Sciences, Hatfield, Pennsylvania) in ice-cold slicing
174 media with 95% O₂/5% CO₂.

175 The organotypic slices were placed on a fine nylon mesh supported on a U-shaped
176 platinum wire in a 35-mm round Petri dish. To achieve air-liquid interface, 0.8 ml sterile filtered
177 culture media (1:1 F12/DMEM, 1% penicillin/streptomycin, 1.2% 6 mg/ml glucose in DMEM,
178 10% fetal bovine serum, and 1% L-glutamine) was added. After the slice cultures were
179 incubated in a humidified incubator (37° C, 5% CO₂) for 1hr, sister cultures were randomly
180 replenished with culture medium containing: (1) 6.5 mM EtOH, (2) 20 μM nifedipine, (3) 6.5 mM
181 EtOH + 20 μM nifedipine, (4) 0.02% DMSO. We used this low concentration of ethanol for the
182 organotypic slice culture experiment as it is equivalent to the blood alcohol concentration (30
183 mg/dL) observed in a mouse model of a low level of chronic ethanol consumption used in
184 previous studies (Cuzon et al., 2008; Skorput and Yeh, 2016).

185 24 hours post-incubation, the slice cultures were washed in PBS and immerse-fixed in
186 4% paraformaldehyde/0.1M phosphate-buffered saline (PBS) overnight at 4°C. Following
187 cryoprotection in 30% sucrose/0.1M PBS, the slice cultures were mounted on charged slides
188 and coverslipped with FluorSave Reagent (Calbiochem, La Jolla, CA).

189

190 *Electrophysiology*

191 On E16.5, pregnant dams were euthanized with CO₂ asphyxiation and fetuses were
192 removed by caesarian section. UV goggles were used to visualize Nkx2.1Cre/Ai14 embryos,
193 which express tdTomato fluorescence in the cortical regions. The brains expressing tdTomato
194 fluorescence were dissected in ice-cold oxygenated artificial cerebrospinal fluid (aCSF)
195 containing (in mM): 125 NaCl, 2.5 KCl, 1 MgCl₂, 1.25 NaH₂PO₄, 2 CaCl₂·2H₂O, 25 NaHCO₃, 25
196 D-glucose, pH 7.4 (adjusted with NaOH). The brains were embedded in 3.8% low-melting point
197 agarose (Invitrogen, Carlsbad, CA). Coronal telencephalic slices (250-μm) containing the
198 embryonic mPFC were obtained using a vibratome (Electron Microscopy Services, Hatfield, PA)
199 and immersed in cutting solution containing (in mM): 3 KCl, 7 MgCl₂, 1.25 NaH₂PO₄, 0.5 CaCl₂,
200 28 NaHCO₃, 5 D-glucose, 110 sucrose, pH 7.4 (adjusted with 1 N NaOH). The slices were then
201 stored in a reservoir of aCSF at room temperature. Only slices from the rostral telencephalon
202 with the embryonic mPFC clearly discernable were used for recording.

203 An acute 250-μm telencephalic slice was transferred to a recording chamber and
204 stabilized by a platinum ring strung with thin plastic threads. The slice was maintained at 34 °C
205 on a heated stage fit onto a fixed-stage upright microscope (BX51WI, Olympus, Melville, NY)
206 and was perfused at a rate of 0.5-1.0 ml/min with oxygenated aCSF. Nkx2.1+ GINs were
207 identified using a 40X water immersion objective (Olympus, Melville, NY) under fluorescence
208 illumination and Hoffman Modulation Optics (Modulation Optics, Greenvale, NY). Images were
209 displayed on a computer monitor through a video camera (Integral Technologies, Indianapolis,
210 IN), which aided the navigation and placement of the recording and drug pipettes.

211 Recording pipettes for whole-cell patch clamp recording were pulled from borosilicate
212 glass capillaries (1.5 mm outer diameter, 0.86 mm inner diameter; Sutter Instrument Co.,
213 Novato, CA). The pipettes were back-filled with KCl internal-solution containing (in mM): 140
214 KCl, 2 CaCl₂, 2 MgCl₂, 11 EGTA, 10 HEPES, pH 7.4. The patch pipettes had resistances of 8-
215 10 MΩ. Recordings were made using an AxoPatch 700B amplifier (Molecular Devices Inc.,
216 Sunnyvale, CA). Membrane currents were digitized at 20 kHz (Digidata 1320A; Molecular
217 Devices), recorded with low-pass filtering at 10 kHz. Recordings were analyzed offline using
218 Mini Analysis (Synaptosoft) and Clampfit 10.3 (Skorput et al., 2019).

219 Nifedipine, TEA, and TTX were dissolved in aCSF immediately prior to recording to a
220 working concentration of 20 μM, 20 mM, and 1 μM, respectively. Ethanol was prepared fresh by
221 diluting 95% ethanol with aCSF to 18 mM for the electrophysiological experiments, which is
222 equivalent to the blood alcohol concentration of 80 mg/dl blood alcohol level attained in the
223 binge-ethanol exposure paradigm used in this and previous studies (Skorput et al., 2015,
224 Skorput et al., 2019).

225 Drug solutions were loaded into separate barrels of a 8-barrel drug pipette assembly that
226 was placed within 10 μm of the soma of the cell under study and applied using regulated pulses
227 of pressure (≤ 3 p.s.i.; Picospritzer, General Valve Corporation, Fairfield, NJ). The timing and
228 duration of the pressure pulses were controlled by a multi-channel timing unit and pulse
229 generator (Pulsemaster A300, WPI, Sarasota, FL). One of the barrels of the multi-barrel drug
230 pipette was filled with aCSF, which was applied between drug applications to clear drugs from
231 the vicinity of the cell and to control for mechanical artifacts that can occur due to bulk flow.

232

233 *Processing of embryonic tissues*

234 Time-pregnant dams were euthanized by CO₂ asphyxiation on E16.5, following control,
235 ethanol (5% w/w), nifedipine (0.15 mg/kg body weight) + ethanol (5% w/w), or nifedipine (0.15

236 mg/kg body weight) treatment. The embryos were removed, their brains dissected, and
237 immerse-fixed in 4% PFA/0.1M PBS overnight at 4°C. Following cryoprotection in 30%
238 sucrose/0.1M PBS overnight, 30- μ m cryosections were cut with a sliding microtome. The slices
239 were mounted on charged glass slides, DAPI counterstained, and coverslipped with FluorSave
240 Reagent (Calbiochem, La Jolla, CA).

241 For immunohistochemistry, 30- μ m coronal sections were collected into PBS and washed
242 overnight at 4° C. The sections were then blocked for 30 minutes at room temperature in PBS
243 containing 10% NGS and 0.025% Triton X-100. The sections were then incubated overnight at
244 4° C with rabbit anti-Cav1.2 primary antibody (Alomone Labs) at a dilution of 1:400 in PBS. The
245 sections were washed in PBS 2X and incubated overnight with a 1:1000 dilution of Alexa Fluor
246 488 conjugated goat-anti-rabbit secondary antibody (Invitrogen, Grand Island, NY) in PBS.
247 Negative control without primary antibody was routinely processed in parallel.

248

249 *Immunofluorescence imaging and analysis*

250 Fluorescent images were acquired using a CCD camera (Hamamatsu, Hamamatsu city,
251 Japan) fit onto a spinning disk confocal microscope (BX61WI; Olympus, Melville, NY) and
252 CellSens software (Olympus). Images were montaged using Photoshop to yield a full view of
253 the region of interest.

254 For each embryonic brain, 10 consecutive sections of the embryonic mPFC beginning at
255 equivalent rostral-caudal levels were imaged and analyzed for counts of Nkx2.1+ GINs. For
256 each litter, sections from a minimum of 3 brains were imaged. The embryonic mPFC was
257 delineated as part of the dorsomedial telencephalon based on DAPI counterstaining of the
258 sections used for analyzing cells. Nkx2.1+ GINs were manually counted using Fiji's cell
259 counting tool by trained experimenters blinded to the experimental condition.

260 For organotypic slice cultures, images were montaged with Photoshop to allow
261 visualization of the cortex throughout its thickness, from the corticostriate juncture (CSJ) to the

262 dorsal apex. One 200- μ m bin immediately proximal to the CSJ, was delineated as one of the
263 regions of interest. Distal to the CSJ, five consecutive 100- μ m bins spanning the thickness of
264 the cortex were organized (Cuzon et al., 2006). The Nkx2.1+ GINs were manually quantified by
265 trained experimenters blinded to the experimental condition using Fiji's cell counting tool. Cell
266 counts in each 100- μ m bin were normalized by counts from the 200- μ m bin proximal to the CSJ
267 from each tissue to calculate the crossing index (Cuzon et al., 2006).

268

269 *Statistics*

270 For histological analyses, n represents the number of litters to minimize litter effects. All
271 groups of histological data were acquired from ten 30- μ m tissue sections per animal from a
272 minimum of three individual animals from multiple litters. For electrophysiological experiments, n
273 also refers to the number of litters used. All statistical analyses were conducted using GraphPad
274 Prism (Version 5.0). Power calculations were performed using the G*Power 3.1 software
275 depending on whether the data were analyzed using t-test or ANOVA. Variance and expected
276 differences were estimated by using group means and standard deviations from preliminary
277 data or past experience in similar studies and reviews of related use in the literature. Group
278 means were compared by paired t-test, one-way ANOVA or two-way ANOVA with appropriate
279 post-hoc test as indicated, and reported in Results as mean (x) \pm standard error.

280

281 **Results**

282 *Binge exposure to ethanol does not affect Cav1.2 expression levels in the embryonic prefrontal*
283 *cortex*

284 We first asked whether LTCCs are expressed in Nkx2.1+ GINs as they migrate
285 tangentially and become positioned in the cortical plate of the embryonic mPFC.

286 Immunohistochemical staining of Cav1.2 in sections from Nkx2.1Cre-Ai14 mouse at E16.5
287 showed that virtually all cells express Cav1.2, including the Nkx2.1+ GINs (Fig. 1). We then

288 assessed if prenatal ethanol exposure alters the expression levels of Cav1.2 in the embryonic
289 medial prefrontal cortex. To this end, pregnant dams were fed liquid diet containing 5% ethanol
290 or isocaloric control from E13.5-E16.5. Embryonic brains dissected at E16.5 were stained for
291 Cav1.2, and immunofluorescence intensity of Cav1.2 and tdTomato was measured using a
292 spinning disk confocal microscope. Fluorescence intensity of Cav1.2 was normalized to that of
293 tdTomato, which is expressed uniformly in the Nkx2.1Cre-Ai14 mice. There was no difference
294 between the fluorescence intensity ratio between control and ethanol-treated embryos at E16.5,
295 indicating that the binge exposure paradigm does not alter the expression levels of Cav1.2 (Fig.
296 2; Control; 1.07 ± 0.08 , n = 4 litters; Ethanol; 1.00 ± 0.027 , n = 5 litters; unpaired t-test,
297 $P > 0.999$).

298

299 *Nifedipine co-treatment in vitro prevents the ethanol-induced aberrant tangential migration*

300 To determine the involvement of LTCCs in ethanol-induced aberrant tangential
301 migration, organotypic slice cultures containing the embryonic mPFC were prepared from E14.5
302 Nkx2.1Cre-Ai14 brains. The slices were incubated in either control or 6.5 mM ethanol-containing
303 medium without or with 20 μ M nifedipine. Following 27 hours of incubation, the slices were fixed
304 in 4% paraformaldehyde/PBS and tangential migration of MGE-derived interneurons was
305 subsequently assessed by counting the number of cells in consecutive 100- μ m bins in the
306 mPFC beginning at the CSJ. The number of cells in each bin was normalized to the number of
307 cells in the 200- μ m bin delineated immediately proximal to the CSJ to calculate the crossing
308 index (Figure 3A). When the number of Nkx2.1+ GINs per 100- μ m bin was compared among
309 the different treatment groups, ethanol-treated organotypic slice cultures had significantly higher
310 number of cells compared to those in the control group (Fig. 3B; Vehicle; 216.9 ± 26.69 cells n =
311 8 cultures, EtOH 319.6 ± 33.54 cells, n = 9 cultures, one-way ANOVA, Tukey's post-hoc test,
312 $p < 0.05$). On the other hand, the number of Nkx2.1+ GINs in the organotypic cultures co-treated
313 with LTCC blocker nifedipine and ethanol were similar to that of control (Nifed + EtOH; $216.1 \pm$

314 14.71 cells, $n = 10$ cultures, $p > 0.999$). At the concentration of nifedipine used ($20 \mu\text{M}$), treatment
315 with the LTCC blocker alone did not alter the density of Nkx2.1+ GINs in the cortex compared to
316 controls (Nifed; 207.2 ± 24.69 , 6 cultures; $P > 0.999$). When the crossing index was analyzed with
317 two-way ANOVA, the number of Nkx2.1+ GINs was significantly higher in ethanol treated
318 cultures compared to control in cortical regions more distal to the CSJ (Fig. 3C). Cultures
319 treated with nifedipine alone and those co-treated with nifedipine and ethanol resulted in a
320 similar crossing index as that of control in all bins. These results implicate calcium flux through
321 the LTCCs being involved in the ethanol-induced aberrant tangential migration, and that
322 blocking LTCCs with nifedipine can normalize the effect of ethanol.

323

324 *Nifedipine co-treatment in vivo prevents the ethanol-induced aberrant tangential migration*

325 To investigate if the preventive effect of nifedipine when co-treated with ethanol seen *in*
326 *vitro* can be replicated *in vivo*, we fed pregnant dams harboring Nkx2.1Cre-Ai14 embryos with a
327 liquid diet containing ethanol (5% EtOH w/w) as well as nifedipine (0.15 mg/kg body weight
328 dissolved in DMSO) from E13.5 - E16.5 according to the timeline outlined in Figure 4A. The
329 dose of nifedipine we used was based on the medical dose of 10 mg prescribed to pregnant
330 women for emergency hypertension and that of the average body weight for first trimester
331 pregnant women is 79 kg (ACOG Committee Opinion No. 767: "Emergent Therapy for Acute-
332 Onset, Severe Hypertension During Pregnancy and the Postpartum Period", 2019). On E16.5,
333 we analyzed the number of Nkx2.1+ GINs in the embryonic mPFC of the progeny (Fig. 4B and
334 C). The laminar localization of these neurons in the embryonic mPFC was not systematically
335 analyzed. Ethanol treatment significantly increased the number of Nkx2.1+ GINs in the mPFC
336 (Fig. 4C; Control; 190.9 ± 22.87 cells, $n = 6$ litters, EtOH; 369.3 ± 3.063 cells, one-way ANOVA,
337 Tukey's post-hoc test, $p < 0.0005$, $n = 3$ litters). Nifedipine treatment during the binge-exposure to
338 alcohol attenuated the number of Nkx2.1+ GINs to a level similar to that of control (Nifed +

339 EtOH; 173.0 ± 24.20 cells; $p > 0.99$, $n = 4$ litters). Nifedipine alone, at the concentration used in
340 this study, did not alter the tangential migration of GABAergic interneurons into the mPFC
341 compared to controls (Nifed; 102.4 ± 27.88 cells; $p > 0.99$, $n = 4$ litters). Thus, the effect of
342 nifedipine in preventing the ethanol-induced enhancement of Nkx2.1+ GINs seen *in vitro* in
343 organotypic slices is recapitulated *in vivo*.

344

345 *Ethanol exposure increases L-type calcium channel activity*

346 We next assessed whether ethanol exposure directly affects LTCC-activated currents in
347 tangentially migrating GABAergic interneurons. We performed whole-cell patch clamp
348 recordings from Nkx2.1+ GINs in acute slices from the embryonic (E16.5) Nkx2.1/Ai14 mouse
349 brains. A multi-barrel drug pipette was used to focally apply 18 mM ethanol, 20 μ M nifedipine, 1
350 μ M TTX, 20 mM TEA, and aCSF to cells being recorded from (Fig. 5A). Calcium current
351 mediated by LTCCs was isolated by applying a depolarizing +40 mV voltage step from a holding
352 potential of -60 mV. Nifedipine application blocked 65.35% of the inward current (Fig. 5C,
353 control; 37.49 ± 7.025 , nifedipine; 12.99 ± 3.240 , $n = 7$ litters, $p < 0.01$). The inward current
354 mediated through nifedipine-sensitive LTCCs was isolated by subtracting the current recorded
355 in presence of nifedipine from that without nifedipine. This current was measured again before
356 and during acute 18mM ethanol application (Fig. 5B). We found that acute ethanol exposure
357 potentiated the LTCC-activated current amplitude by 33.16% (Fig. 5D, Control; 27.31 ± 7.158 ,
358 Ethanol; 40.86 ± 11.81 , $n = 7$ litters, paired t-test, $p < 0.05$). These results indicate that ethanol
359 augments LTCC-mediated currents in embryonic Nkx2.1+ GINs and, thus, calcium influx
360 consequent to an ethanol-induced potentiation of GABA_A receptor-mediated depolarization
361 (Skorput et al., 2019).

362

363 **Discussion**

364 We sought to contribute to elucidating the mechanisms underlying the embryonic
365 etiology of FASD in this study. This was motivated by our previous studies that showed ethanol
366 altering tangential migration of GABAergic interneurons (Cuzon et al., 2008; Skorput et al. 2015;
367 Skorput et al. 2019). The major findings of this study are three-fold. First, we showed that
368 Cav1.2 (or α_{1c}) is ubiquitously expressed in the embryonic mouse cortex. Second, nifedipine,
369 presented either directly to organotypic slices *in vitro* or through *in vivo* treatment of ethanol-
370 consuming pregnant dams, prevents the ethanol-induced aberrant tangential migration in the
371 fetal cortex. Third, we provide evidence that ethanol enhances calcium influx through LTCCs in
372 migrating embryonic GABAergic interneurons. Collectively, these findings provide evidence for
373 calcium and LTCCs being important regulators of the ethanol-induced aberrant tangential
374 migration of GINs in the embryonic mPFC.

375 Figure 6 integrates the results of the present study and those of a recent one (Skorput et
376 al., 2019) that, together, led to formulating an LTCC-based subcellular mechanistic scheme by
377 which ethanol may mobilize tangential migration in embryonic GINs. Under normal control
378 conditions (Fig. 6A), the preponderance of the NKCC1 chloride importer vis-à-vis the KCC2
379 chloride exporter generates a net high intracellular level of chloride that maintains a depolarized
380 membrane potential in embryonic GINs. In addition, tonic activation of GABA_A receptors by an
381 ambient presence of GABA in the extracellular milieu (Cuzon et al., 2006) leads to a net chloride
382 efflux and depolarization of the membrane. Ethanol exposure (Fig. 6B) does not directly affect
383 the action of the NKCC1 cotransporter but potentiates chloride efflux through GABA_A receptors,
384 resulting in enhanced depolarization (Skorput et al., 2019) which goes on to promote
385 downstream processes that either enhance LTCC activity (Fig. 6B) or trigger other mechanisms
386 that increase intracellular calcium dynamics. One such mechanism, as postulated in Figure 6,
387 may be a surrogate activation of the calcium-permeable NMDA receptors following the
388 depolarization-dependent release of the magnesium block. Whether and how such surrogate

389 interacts and comes into play in conferring ethanol's influence on the tangential migration of
390 cortical GINs await experimental elucidation.

391 Our results indicate that, although the embryonic neocortex expresses Cav1.2, or α_{1c} , at
392 E16.5, prenatal exposure to ethanol did not affect Cav1.2 expression levels in the embryonic
393 prefrontal cortex. It should be noted that this finding deviates from earlier studies in which
394 chronic ethanol exposure was shown to increase calcium uptake through LTCCs, presumably
395 through the increase in expression of α_1 and α_2/δ_1 subunits of LTCCs in cortical neurons and
396 α_{1c} , α_2 , and β_{1b} in neural crest-derived cell line PC12 (Katsura et al., 2006; Walter et al., 2000).
397 A parsimonious explanation to account for the apparent discrepant results regarding LTCC
398 expression might be due to the use of high doses of ethanol in the previous studies (50-150
399 mM) vis-à-vis the more moderate concentrations of ethanol (6.5 mM and 18 mM) used here. In
400 addition, the earlier studies employed a chronic ethanol exposure paradigm (Katsura et al.,
401 2006; Walter et al., 2000), and this differs from the binge-type ethanol exposure early in
402 gestation employed in our study.

403 Nifedipine treatment in ethanol-exposed organotypic slice cultures prevented the
404 aberrance in tangential migration. Maternal nifedipine treatment along with binge exposure to
405 ethanol also normalized migration disrupted by ethanol *in vivo*. Nifedipine, as a dihydropyridine
406 calcium channel blocker, can have wide-ranging systemic effects, including activation of the
407 reflex sympathetic nervous system, increase in myocardial oxygen supply, and decrease in
408 blood pressure (Gibbons et al., 2003; Abrams et al., 2007). Pregnant mice treated with
409 nifedipine may be subject to such physiological changes, independent of or in addition to its
410 effects on the embryonic central nervous system. However, we favor the prospect that
411 nifedipine's effect on the tangential migration of Nkx2.1+ GINs most likely involves a direct
412 effect, vis-à-vis, secondary effects on physiological alterations, as similar outcomes were
413 recapitulated in our organotypic slice culture experiments that would have arguably
414 circumvented any direct systemic effects.

415 In the present study, acute exposure to ethanol enhanced the activity of LTCCs. We
416 note that acute ethanol exposure has been shown to inhibit the function of LTCCs in several
417 neuronal preparations (Wang et al., 1991; Wang et al., 1994; Mullikin-Kilpatrick and Treisman,
418 1995; Zucca et al., 2010; Mah et al., 2011; Morton et al., 2016). Such differences may arise
419 from the fact that embryonic neurons have relatively depolarized resting membrane potentials
420 (approximately -40 mV; Skorput et al., 2019), such that membrane depolarization exerted by
421 traditionally hyperpolarizing neurotransmitters such as GABA might be more conducive to
422 reaching the activation potential for LTCCs (Nakanishi and Okazawa, 2006; Horigane et al.,
423 2019). We hypothesized that ethanol, by potentiating depolarization through GABA_A receptors,
424 may further activate LTCCs, increasing calcium influx into the migrating embryonic GABAergic
425 interneurons (Fig. 6B). This is in line with reduced calcium signaling observed in tangentially
426 migrating interneurons with KCC2 upregulation, which decreases GABA-induced depolarization
427 (Bortone and Polleux, 2009). In this study, we did not confirm the role of GABA as a mediator of
428 the observed increase in calcium influx through LTCCs. Nonetheless, our findings provide the
429 basis for investigating further the interplay between GABA_A receptor and LTCCs activation in
430 embryonic Nkx2.1+ GINs upon ethanol exposure.

431 L-type calcium channels are predictably not the only voltage-gated calcium channels that
432 immature GABAergic cortical interneurons express. Thus, the involvement of L-type calcium
433 channels does not preclude the role of other voltage-activated calcium channels in regulating
434 the tangential migration of Nkx2.1+ GINs. Ligand-gated ion channels other than GABA_A
435 receptors may also play a role. For example, NMDA receptors are expressed in immature
436 GABAergic cortical interneurons (Soria and Valdeolillos, 2002). Since NMDA receptor
437 activation relies on membrane depolarization-induced release of magnesium block, a GABA-
438 mediated depolarization may facilitate NMDA receptor activation and, thereby, promote calcium
439 influx in immature GABAergic interneurons. This surrogate activation of NMDA receptors may
440 be augmented with ethanol exposure (Fig. 6). Future investigative work will need to confirm the

441 potential involvement of NMDA and interplay with GABA_A receptor activation in this mechanistic
442 signaling scheme.

443 The present study demonstrated that ethanol increases LTCC-mediated channel activity
444 (Fig. 6B). However, how this would enhance tangential migration of cortical GABAergic
445 interneurons still remains unresolved. Calcium signaling is critical in activating the downstream
446 cytoskeletal dynamics in mechanisms underlying neuronal migration (Gomez and Spitzer, 1999;
447 Lautermilch and Spitzer, 2000; Gomez et al., 2001; Wen et al., 2004; Kerstein, Patel, and
448 Gomez, 2017). Live imaging studies addressing changes in filopodia motility, somal
449 translocation, or trailing tail retraction, as downstream mechanisms of ethanol-induced
450 potentiation of LTCC-mediated calcium current will further elucidate how ethanol affects normal
451 tangential migration of primordial GABAergic cortical interneurons and, thus, contribute to our
452 understanding of the pathoetiology of FASD.

453 While the diagnosis of FASD occurs postnatally, its embryonic etiology is
454 incompletely understood. The current study focused on investigating how ethanol as a
455 teratogen disrupts the process of migration in the embryonic neocortex. We demonstrated
456 that ethanol increases chloride efflux to enhance GABA-induced depolarization, and
457 increases LTCC activity in migrating interneurons. Ethanol may also activate NMDA
458 receptors, which are calcium permeable, and enhanced activation of voltage-gated calcium
459 channels may increase calcium influx into the cell, which may act on downstream targets to
460 alter cytoskeletal dynamics. Overall, data presented here point to LTCCs playing an
461 important role in the ethanol-induced aberrant tangential migration of cortical GABAergic
462 interneurons. We propose that the inhibition of LTCCs by nifedipine, as an FDA approved
463 drug, may bear therapeutic potential in treating and managing FASD.

464

465 **References**

- 466 Abrams J, Schroeder J, Frishman WH, Freedman J. 2007. Pharmacologic Options for
467 Treatment of Ischemic Disease. *Cardiovascular Therapeutics*. doi:10.1016/b978-1-4160-
468 3358-5.50011-5
- 469 ACOG Committee Opinion No. 767: Emergent Therapy for Acute-Onset, Severe Hypertension
470 During Pregnancy and the Postpartum Period. 2019. . *Obstet Gynecol* 133:e174–e180.
- 471 American Academy of Pediatrics. Committee on Substance Abuse and Committee on Children
472 With Disabilities. Fetal alcohol syndrome and alcohol-related neurodevelopmental
473 disorders. 2000. . *Pediatrics* 106:358–361.
- 474 Bortone D, Polleux F. 2009. KCC2 expression promotes the termination of cortical interneuron
475 migration in a voltage-sensitive calcium-dependent manner. *Neuron* 62:53–71.
- 476 Carr JL, Agnihotri S, Keightley M. 2010. Sensory processing and adaptive behavior deficits of
477 children across the fetal alcohol spectrum disorder continuum. *Alcohol Clin Exp Res*
478 34:1022–1032.
- 479 Clancy B, Darlington RB, Finlay BL. 2001. Translating developmental time across mammalian
480 species. *Neuroscience*. 105:7-17
- 481 Cross-Disorder Group of the Psychiatric Genomics Consortium. 2013. Identification of risk loci
482 with shared effects on five major psychiatric disorders: a genome-wide analysis. *Lancet*
483 381:1371–1379.
- 484 Cuzon VC, Yeh PW, Cheng Q, Yeh HH. 2006. Ambient GABA promotes cortical entry of
485 tangentially migrating cells derived from the medial ganglionic eminence. *Cereb Cortex*
486 16:1377–1388.
- 487 Cuzon VC, Yeh PWL, Yanagawa Y, Obata K, Yeh HH. 2008. Ethanol consumption during early
488 pregnancy alters the disposition of tangentially migrating GABAergic interneurons in the
489 fetal cortex. *J Neurosci* 28:1854–1864.

- 490 Danesi C, Achuta VS, Corcoran P, Peteri U-K, Turconi G, Matsui N, Albayrak I, Rezov V,
491 Isaksson A, Castrén ML. 2018. Increased Calcium Influx through L-type Calcium Channels
492 in Human and Mouse Neural Progenitors Lacking Fragile X Mental Retardation Protein.
493 *Stem Cell Reports* 11:1449–1461.
- 494 Darcy DP, Isaacson JS. 2009. L-type calcium channels govern calcium signaling in migrating
495 newborn neurons in the postnatal olfactory bulb. *J Neurosci* 29:2510–2518.
- 496 Delatour LC, Yeh PWL, Yeh HH. 2019. Ethanol exposure in utero disrupts radial migration and
497 pyramidal cell development in the somatosensory cortex. *Cereb Cortex* 29:2125–2139
- 498 Delatour LC, Yeh PWL, Yeh HH. 2020. Prenatal Exposure to Ethanol Alters Synaptic Activity in
499 Layer V/VI Pyramidal Neurons of the Somatosensory Cortex. *Cereb Cortex* 30:1735–1751.
- 500 England LJ, Bennett C, Denny CH, Honein MA, Gilboa SM, Kim SY, Guy GP Jr, Tran EL, Rose
501 CE, Bohm MK, Boyle CA. 2020. Alcohol Use and Co-Use of Other Substances Among
502 Pregnant Females Aged 12-44 Years - United States, 2015-2018. *MMWR Morb Mortal*
503 *Wkly Rep* 69:1009–1014.
- 504 Floyd RL, Decouflé P, Hungerford DW. 1999. Alcohol use prior to pregnancy recognition. *Am J*
505 *Prev Med* 17:101–107.
- 506 Gibbons RJ, Abrams J, Chatterjee K, Daley J, Deedwania PC, Douglas JS, Ferguson TB Jr,
507 Fihn SD, Fraker TD Jr, Gardin JM, O'Rourke RA, Pasternak RC, Williams SV, American
508 College of Cardiology, American Heart Association Task Force on practice guidelines
509 (Committee on the Management of Patients With Chronic Stable Angina). 2003. ACC/AHA
510 2002 guideline update for the management of patients with chronic stable angina--
511 summary article: a report of the American College of Cardiology/American Heart
512 Association Task Force on practice guidelines (Committee on the Management of Patients
513 With Chronic Stable Angina). *J Am Coll Cardiol* 41:159–168.
- 514 Gomez TM, Robles E, Poo M, Spitzer NC. 2001. Filopodial calcium transients promote
515 substrate-dependent growth cone turning. *Science* 291:1983–1987.

- 516 Gomez TM, Spitzer NC. 1999. In vivo regulation of axon extension and pathfinding by growth-
517 cone calcium transients. *Nature* 397:350–355.
- 518 Horigane S-I, Ozawa Y, Yamada H, Takemoto-Kimura S. 2019. Calcium signalling: a key
519 regulator of neuronal migration. *J Biochem* 165:401–409.
- 520 Idänpään-Heikkilä J, Jouppila P, Akerblom HK, Isoaho R, Kauppila E, Koivisto M. 1972.
521 Elimination and metabolic effects of ethanol in mother, fetus, and newborn infant. *Am J*
522 *Obstet Gynecol* 112:387–393.
- 523 Inada H, Watanabe M, Uchida T, Ishibashi H, Wake H, Nemoto T, Yanagawa Y, Fukuda A,
524 Nabekura J. 2011. GABA regulates the multidirectional tangential migration of GABAergic
525 interneurons in living neonatal mice. *PLoS One* 6:e27048.
- 526 Kabir ZD, Martínez-Rivera A, Rajadhyaksha AM. 2017. From Gene to Behavior: L-Type Calcium
527 Channel Mechanisms Underlying Neuropsychiatric Symptoms. *Neurotherapeutics* 14:588–
528 613.
- 529 Kamijo S, Ishii Y, Horigane S-I, Suzuki K, Ohkura M, Nakai J, Fujii H, Takemoto-Kimura S, Bito
530 H. 2018. A Critical Neurodevelopmental Role for L-Type Voltage-Gated Calcium Channels
531 in Neurite Extension and Radial Migration. *J Neurosci* 38:5551–5566.
- 532 Katsura M, Shibasaki M, Hayashida S, Torigoe F, Tsujimura A, Ohkuma S. 2006. Increase in
533 Expression of $\alpha 1$ and $\alpha 2/\delta 1$ Subunits of L-Type High Voltage-Gated Calcium Channels
534 After Sustained Ethanol Exposure in Cerebral Cortical Neurons. *J Pharmacol Sci* 102:221–
535 230.
- 536 Kerstein PC, Patel KM, Gomez TM. 2017. Calpain-Mediated Proteolysis of Talin and FAK
537 Regulates Adhesion Dynamics Necessary for Axon Guidance. *J Neurosci* 37:1568–1580.
- 538 Komuro H, Rakic P. 1998. Orchestration of neuronal migration by activity of ion channels,
539 neurotransmitter receptors, and intracellular Ca^{2+} fluctuations. *J Neurobiol* 37:110–130.
- 540 Komuro H, Rakic P. 1996. Intracellular Ca^{2+} fluctuations modulate the rate of neuronal
541 migration. *Neuron* 17:275–285.

- 542 Lautermilch NJ, Spitzer NC. 2000. Regulation of calcineurin by growth cone calcium waves
543 controls neurite extension. *J Neurosci* 20:315–325.
- 544 Mattson SN, Crocker N, Nguyen TT. 2011. Fetal alcohol spectrum disorders:
545 neuropsychological and behavioral features. *Neuropsychol Rev* 21:81–101.
- 546 Mah SJ, Fleck MW, Linsley TA. 2011 Ethanol alters calcium signaling in axonal growth cones.
547 *Neuroscience*. 189:384-396
- 548 Morton RA, Valenzuela CF. 2016. Further characterization of the effect of ethanol on voltage-
549 gated Ca²⁺ channel function in developing CA3 hippocampal pyramidal neurons. *Brain*
550 *Res*. 1633:19-26
- 551 Moya F, Valdeolillos M. 2004. Polarized increase of calcium and nucleokinesis in tangentially
552 migrating neurons. *Cereb Cortex* 14:610–618.
- 553 Mullikin-Kilpatrick D, Treistman SN. 1995. Inhibition of dihydropyridine-sensitive Ca⁺⁺ channels
554 by ethanol in undifferentiated and nerve growth factor-treated PC12 cells: interaction with
555 the inactivated state. *J Pharmacol Exp Ther* 272:489–497.
- 556 Nakanishi S, Okazawa M. 2006. Membrane potential-regulated Ca²⁺ signalling in development
557 and maturation of mammalian cerebellar granule cells. *J Physiol* 575:389–395.
- 558 Parnell SE, Holloway HE, Baker LK, Styner MA, Sulik KK. 2014. Dysmorphogenic effects of first
559 trimester equivalent ethanol exposure in mice: a magnetic resonance microscopy-based
560 study. *Alcohol Clin Exp Res* 28:2008-2014
- 561 Roozen S, Peters G-JY, Kok G, Townend D, Nijhuis J, Curfs L. 2016. Worldwide prevalence of
562 fetal alcohol spectrum disorders: A systematic literature review including meta-analysis.
563 *Alcohol Clin Exp Res* 40:18–32.
- 564 Skorput AGJ, Gupta VP, Yeh PWL, Yeh HH. 2015. Persistent Interneuronopathy in the
565 Prefrontal Cortex of Young Adult Offspring Exposed to Ethanol In Utero. *Journal of*
566 *Neuroscience*. doi:10.1523/jneurosci.1462-15.2015

- 567 Skorput AG, Lee SM, Yeh PW, Yeh HH. 2019. The NKCC1 antagonist bumetanide mitigates
568 interneuronopathy associated with ethanol exposure in utero. *Elife* 8.
569 doi:10.7554/eLife.48648
- 570 Soria JM, Valdeolmillos M. 2002. Receptor-activated calcium signals in tangentially migrating
571 cortical cells. *Cereb Cortex* 12:831–839.
- 572 Walter HJ, McMahon T, Dadgar J, Wang D, Messing RO. 2000. Ethanol Regulates Calcium
573 Channel Subunits by Protein Kinase C δ -dependent and -independent Mechanisms.
574 *Journal of Biological Chemistry*. doi:10.1074/jbc.m910282199
- 575 Wang XM, Dayanithi G, Lemos JR, Nordmann JJ, Treistman SN. 1991. Calcium currents and
576 peptide release from neurohypophysial terminals are inhibited by ethanol. *J Pharmacol Exp*
577 *Ther* 259:705–711.
- 578 Wang X, Wang G, Lemos JR, Treistman SN. 1994. Ethanol directly modulates gating of a
579 dihydropyridine-sensitive Ca²⁺ channel in neurohypophysial terminals. *J Neurosci*
580 14:5453–5460.
- 581 Wen Z, Guirland C, Ming G-L, Zheng JQ. 2004. A CaMKII/Calcineurin Switch Controls the
582 Direction of Ca²⁺-Dependent Growth Cone Guidance. *Neuron* 43:835–846.
- 583 Yang S, Huang X-Y. 2005. Ca²⁺ influx through L-type Ca²⁺ channels controls the trailing tail
584 contraction in growth factor-induced fibroblast cell migration. *J Biol Chem* 280:27130–
585 27137.
- 586 Zucca S, Valenzuela CF. 2010 Low concentrations of alcohol inhibit BDNF-dependent
587 GABAergic plasticity via L-type Ca²⁺ channel inhibition in developing CA3 hippocampal
588 pyramidal neurons. *J Neurosci* 30 (19) 6776-6781
589

590 **Figure Legends**

591

592 **Figure 1. Cav1.2 is expressed in the embryonic medial prefrontal cortex.**

593 (A) Representative images of histological sections from Nkx2.1/Ai14 E16.5 mouse brain (A1)
594 immunostained for Cav1.2 (A2) and overlaid with images of DAPI counterstaining and
595 Nkx2.1/tdTomato-fluorescent GABAergic interneurons (A3). Images were captured at 10X
596 magnification on a spinning disk confocal microscope. (B) Representative images at 40X
597 magnification. These images are magnified images of the area demarcated by the white box in
598 A1-A3. (C) Representative images of no primary antibody negative control of Cav1.2 staining.
599

600 **Figure 2. Prenatal ethanol exposure does not alter Cav1.2 expression.**

601 (A) Representative images of Cav1.2 staining overlaid with DAPI and Nkx2.1 in the medial
602 prefrontal cortex (mPFC) of control (A1) and ethanol-fed (A2) E16.5 mouse brain. (B)
603 Quantification of fluorescence intensity ratio of Cav1.2 to Nkx2.1 in the mPFC of control and
604 ethanol-treated mice. Unpaired t-test. See Results for statistical details.

605

606 **Figure 3. Nifedipine prevents ethanol-induced aberrant migration in organotypic slice**
607 **cultures**

608 (A) Representative image of Nkx2.1/Ai14 embryonic mouse brain with 5 bins (100- μ m wide
609 each) above corticostriate juncture (CSJ) and one 200- μ m bin below CSJ. (B) Quantification of
610 mean Nkx2.1+ cells per individual bins in control (Vehicle; 3 litters, 3 females, 5 males), ethanol
611 (EtOH; 3 litters, 6 females, 3 males), ethanol + nifedipine (EtOH + Nifed; 3 litters, 7 females, 3
612 males), and nifedipine (Nifed; 3 litters, 2 females, 4 males) treated organotypic slice cultures.
613 (C) Quantification of crossing index for control (Vehicle), ethanol (EtOH), ethanol + nifedipine
614 (EtOH + Nifed), and nifedipine (Nifed) treated organotypic slice cultures. * compared to control,

615 # compared to EtOH + Nifed. *, # = $p < 0.05$, **, ### = $p < 0.01$, ***, ### = $p < 0.001$, two-way
616 ANOVA with Tukey's post hoc test

617

618 **Figure 4. Maternal nifedipine treatment normalizes ethanol-induced enhancement of**
619 **tangential migration in vivo.**

620 (A) Experimental timeline. Graded blue box highlights the period of tangential migration,
621 beginning at ~E01.5 and tapering out by ~P0. Binge-type ethanol exposure and nifedipine co-
622 treatment begins on E13.5 and ends on E16.5 (red dashed lines). (B) Fluorescent images of
623 mPFC counterstained with DAPI in mice that received control, binge-type maternal ethanol
624 consumption from E13.3 - E16.5 (EtOH), ethanol exposure in combination with maternal
625 nifedipine treatment in liquid diet (0.15 mg/kg body weight) (EtOH+Nifed), or nifedipine only
626 treatment (Nfed). Scale bars = 100 μm . (C) Quantification of Nkx2.1⁺ cells in all treatment
627 groups. ** = $p < 0.01$ compared to control. one-way ANOVA with Tuckey's post hoc test.

628

629 **Figure 5. Ethanol acutely potentiates calcium current mediated by L-type calcium**
630 **channels.**

631 (A) Representative images of the recording setup. Hoffman modulation contrast image of an
632 acute slice from E16.5 mouse brain with the patch clamp recording pipette (A1, right) pointed at
633 a tdTomato-fluorescent Nkx2.1⁺ GABAergic interneuron to be recorded in the whole-cell voltage
634 clamp configuration. A multi-barrel drug pipette is navigated to the vicinity of the cell being
635 recorded (A1, left). (B) Calcium current mediated by L-type voltage-gated calcium channels was
636 isolated by performing 40-mV depolarizing voltage steps in the presence of TTX, TEA (black
637 trace). This current was subtracted with current obtained from 40-mV depolarizing steps in the
638 presence of TTX, TEA, and nifedipine (Nifedipine, gray trace). L-type calcium current was
639 measured again in the presence of 18 mM ethanol (EtOH, red trace). (C) Quantification of peak
640 amplitude of calcium current mediated by LTCC in the presence of TTX and TEA (Control) and

641 nifedipine (Nifedipine). ** = $p < 0.01$ paired t-test. (D) Peak amplitude of calcium current mediated
642 by LTCC in the before (Control) and during acute 18mM ethanol exposure (EtOH). * = $p < 0.05$
643 unpaired t-test

644

645 **Figure 6. Schematic diagram summarizing the effect of ethanol on migrating**
646 **embryonic cortical GABAergic interneurons.** (A) The depolarizing action of GABA in
647 embryonic cortical GINs is established by the predominant expression of NKCC1 chloride
648 importer relative to that of the KCC2 chloride exporter, resulting in heightened intracellular
649 chloride. GABA binding to its cognate GABA_A receptor thus causes chloride efflux and
650 membrane depolarization. (B) Following ethanol exposure, chloride efflux from GABA_A
651 receptors is enhanced, shifting the membrane potential of embryonic GABAergic
652 interneurons to more depolarized levels. This enhanced depolarization of the membrane
653 potential promotes the activation of L-type voltage-gated calcium channels (LTCC). It is
654 postulated that the increased depolarization may also activate NMDA receptors by releasing
655 the voltage-dependent Mg⁺⁺ block. The increase in the activity of calcium-permeable
656 channels may, in turn, increase calcium influx, raising intracellular calcium, and further
657 activate downstream calcium signaling mechanisms. The net result of this chloride-to-
658 calcium interplay mobilizes changes in the actin-microtubule dynamics and promote
659 migration of cortical GABAergic interneurons.

660

661

Figure 1

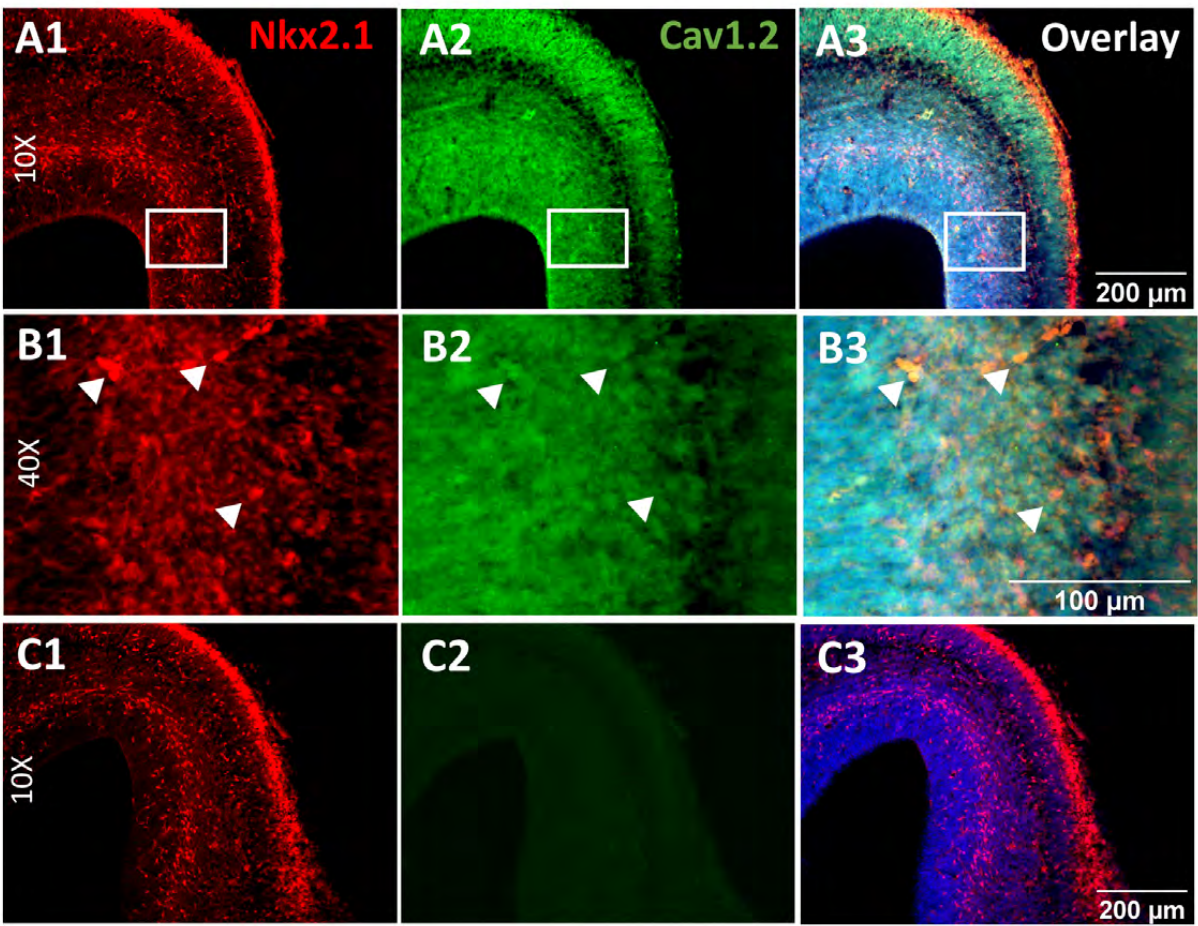


Figure 2

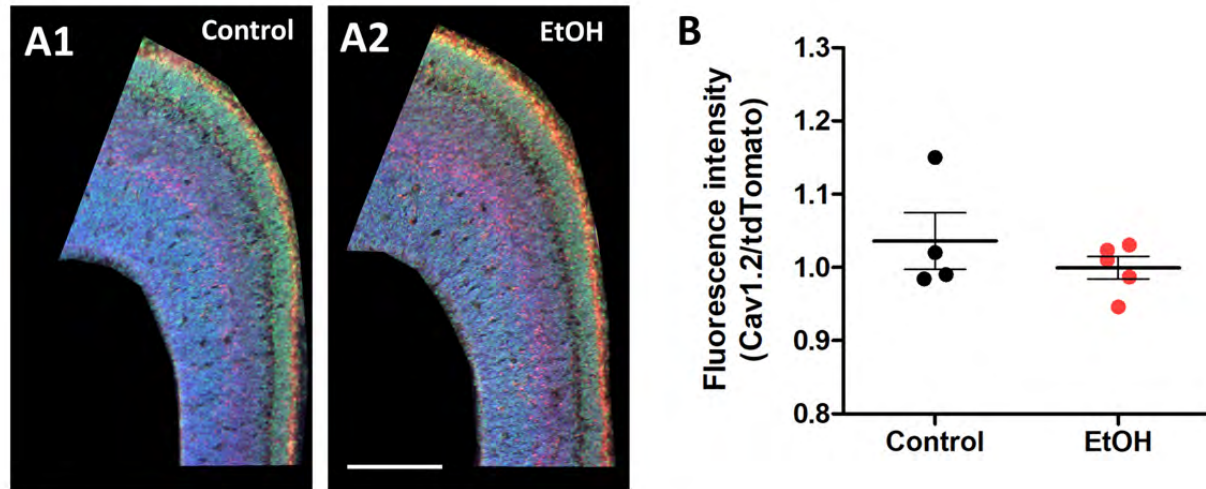
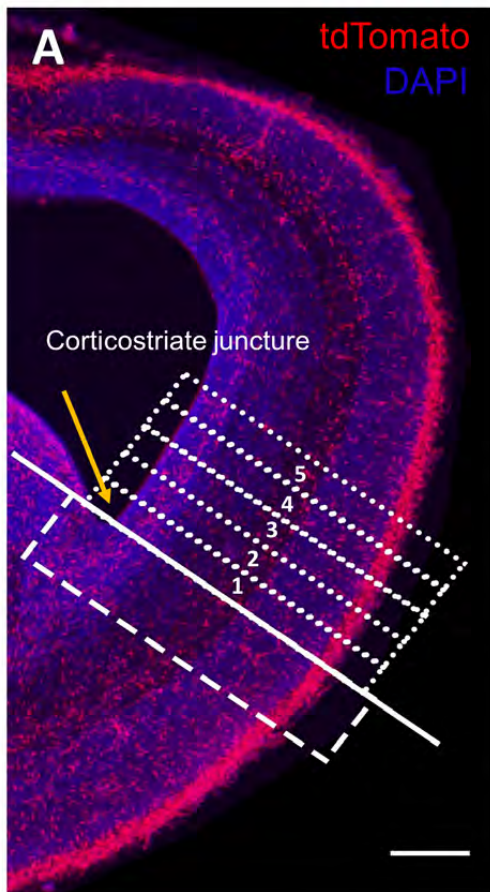
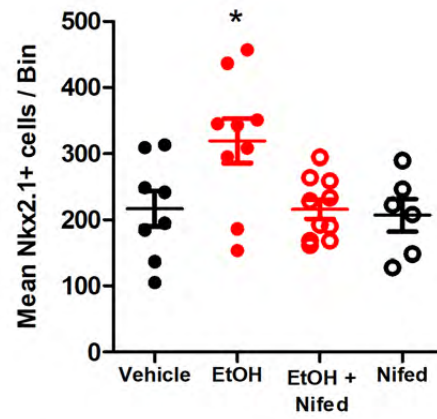


Figure 3



B



C

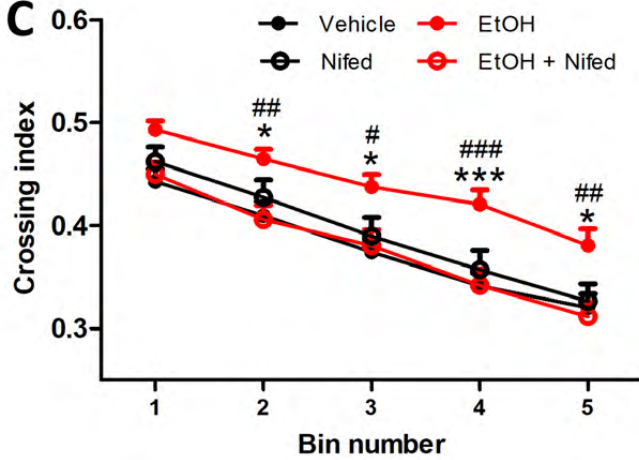


Figure 4

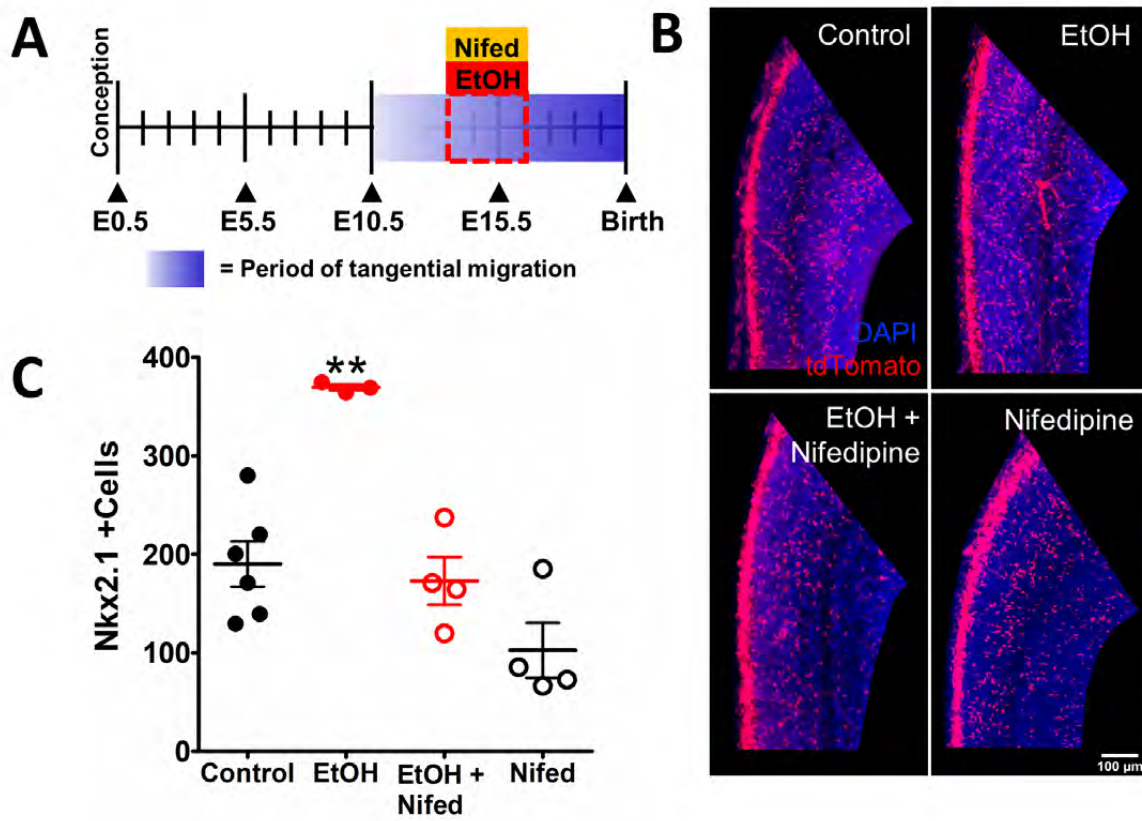


Figure 5

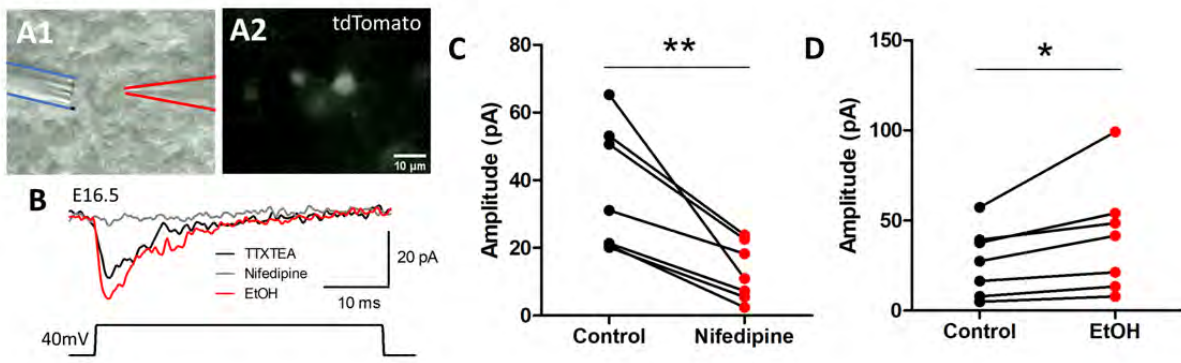


Figure 6

